Mass Effect of a Thyroid Goiter That Crimps the Great Vessels

James D. Collins, MD

Keywords: MRI ■ thyroid goiter ■ anatomy ■ mastectomy ■ costoclavicular compression ■ chest ■ radiology

J Natl Med Assoc. 2011;103:364-369

Author Affiliations: University of California at Los Angeles, Department of Radiological Sciences, Los Angeles, California.
Correspondence: James D. Collins, MD, University of California at Los Angeles, Department of Radiological Sciences, 10833 Le Conte Ave, BL-428 CHS/UCLA mail code 172115, Los Angeles, CA 90095 (jamesc@mednet.ucla.edu).

CLINICAL HISTORY

This is a 70-year-old right-handed female that was being considered for Botox injections because of pain and numbness in the 4 to 5 digits of the right hand after painting walls in her home not described as radicular pain.

She had right arm weakness and a sense of weakness in the right leg and complained of pain down the right trapezius muscle around the right hip and into the groin, where the pain stopped. Her left arm was fine. She had multiple magnetic resonance imaging (MRI) scans, including of the cervical spine.

PAST MEDICAL HISTORY

Her medical history included hyperlipidemia and left mastectomy for left-sided breast cancer about a year before her physical examination.[1]

PAST SURGICAL HISTORY

She had resection for enlarged left thyroid gland 30 years ago and has taken Synthroid for the past 2 years. Other medications included Celebrex, Methadone, Cymbalta, and Fentanyl 50 μg.

REVIEW OF SYSTEMS

Unremarkable except as above.

PHYSICAL EXAMINATION

Blood pressure in the right arm was 130/82 mm Hg; pulse, 60 beats/min; respiration, 18 breaths/min; temperature, 97.9ºF. She was positive for palpable enlarged right thyroid gland displacing the trachea to the left of midline. There was a scar over the site of the left mastectomy. There was no skin or suspicious masses in the right breast.

NEUROLOGICAL EXAMINATION

Her sensory examination indicated her left hand was twice as sensitive to light touch than the right hand. Pin prick was equal. Right lower extremity was not tested. In the right lower extremity, motor strength was good, but there was a sense of give-way weakness, especially in the right iliopsoas muscle. Reflexes were symmetric and brisk at the knees, 2+ in the left ankle, and 1+ 2+ in the right ankle, fairly close but not quite equal. She had weakness of the right hamstring muscles. Adson's maneuver was positive (a test for disappearance of the radial pulse indicating a positive test) in the right upper extremity. Her pulse was weak on the right as compared to the left. The left shoulder sloped more than right side and persisted with shrugging of the shoulders. Deltoid muscle strength appeared comparable bilaterally. Right biceps muscle was slightly weaker than left. Right triceps muscle and wrist extensors were markedly weaker on the right than the left. The right hand intrinsic, ulnar, and median muscles were markedly weaker than on the left. Reflexes in the biceps, triceps, and brachioradialis were completely symmetric.

DIAGNOSIS: THORACIC OUTLET SYNDROME

Because the referring physician was aware of our procedure, he requested bilateral MRI/magnetic resonance angiography (MRA)/magnetic resonance venography (MRV) of the brachial plexus to detect sites of brachial plexus compression.

RADIOGRAPHIC AND MAGNETIC RESONANCE FINDINGS

The posterior-anterior chest radiograph (Figure 1) displays the patient leaning left; anterior-rotated heads of the clavicles over the posterior fourth ribs, left lower than right; drooping left shoulder as compared to the right; multiple metal clips over the left lateral chest wall from mastectomy, posterior fifth through the ninth ribs, accentuating atrophy of the muscles in the left arm as compared to the right and surgical absence of the left

breast and the axillary tail of Spence secondary to left mastectomy; right concave scoliosis of the cervicothoracic spine, C2 through T5; accentuating the concave compression of the trachea to the left of midline by the enlarged right lobe of the thyroid gland, C7 through T5; atheromatous calcifications within the arch of the aorta; cystic bronchiectasis over the region of the inferior lingual segment of the left lung; concave left scoliosis of the thoracolumbar spine, T6 through L1. The lateral chest radiograph (not displayed) showed rounding of the shoulders; kyphosis of the thoracic spine; dense right lobe of the thyroid posterior to the manubrium and inferior to the first ribs; metal clips over the left lateral chest wall marginating the upper trachea and cardiac margins; cystic changes involving the inferior lingular bronchi of the left lung; left breast absence with marginal thickening of the left lower lobe bronchus.

CHEST RADIOGRAPH CONCLUSIONS

- Postresection left thyroid with enlarged lobe of the right thyroid displacing the trachea to the left of midline as above described.
- Post–left mastectomy with atrophy of the left upper arm muscles and chest wall.
- Bilateral round shoulders, left droops as compared to the right.
- Cystic bronchiectasis inferior lingular segment of the left lung.
- Kyphoscoliosis of the cervicothoracolumbar as above described.
- Degenerative changes cervical spine as above described.

Multiplanar MRI cross-referenced the chest radiographs to display the splayed apart crimped great vessels (subclavian, brachiocephalic, and common carotid arteries) (Figure 2) secondary to the combined backward displaced manubrium and the downward-displaced cystic right thyroid gland displacing the trachea and esophagus to the left of midline; compressed inferior bicuspid valve within the right internal jugular vein greater than on the left; asymmetric gray proton-dense external jugular

Figure 1. Posterior-anterior chest view showing the density of the large right lobe of the thyroid (3 small arrows) displacing the trachea (T) left of midline; forward-drooping left shoulder as compared to the elevated right shoulder; anterior-rotated heads of the clavicles (C) over the asymmetric posterior fourth intercostal spaces (not labeled); asymmetric breasts accentuating the radiolucent left hemithorax reflecting left mastectomy; right hemidiaphragm (RD) slightly higher than the left (LD); resected left axillary fold (AS) (axillary tail of Spence) as compared to the right; atrophic left arm muscles (not labeled).

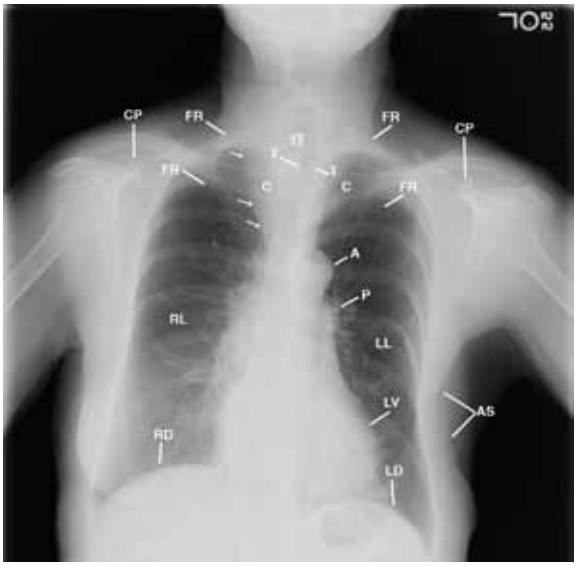

A, aorta; CP, coracoid process; FR, first rib; LL, left lung; 1T, first thoracic vertebra; LV, left ventricle; P pulmonary artery ; RL, right lung.

Figure 2. This is a series of 6 coronal images that display the trachea (T) and esophagus (E) displaced to the left of midline by the gray proton mixed signal intensities of the follicular cystic right lobe of the thyroid (TH); splayed-apart crimped subclavian arteries (SA), common carotid arteries (CC), and brachiocephalic veins (BRV) images 24-25; bulbous expanded inferior bicuspid valve within the right internal jugular vein (J), image 25; degenerative change of the uncovertebral joints inferior to the vertebral body of C5; left lobe of the thyroid (TH) right lateral to the trachea, image 25.

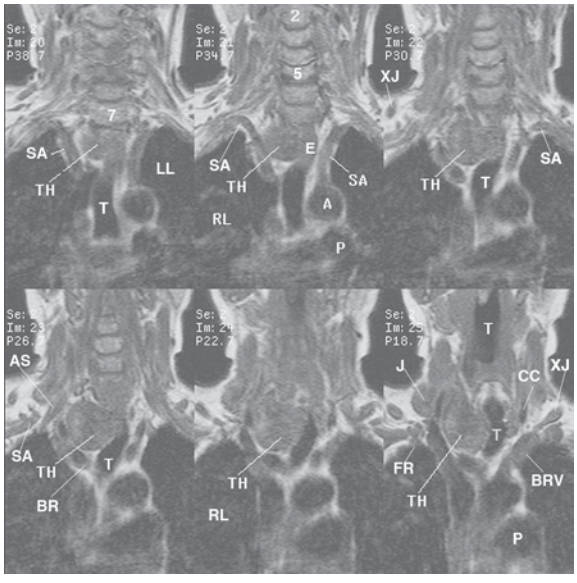

A, aorta; AS, anterior scalene muscle; BR, brachiocephalic artery; C2, C7, cervical vertebra; LL, left lung; P, pulmonary artery; RL, right lung; XJ, external jugular vein.

veins draining over the bulbous expanded compressed subclavian veins on the asymmetric first ribs, left lower than right; atrophy of the soft tissues of the left anterior chest wall (not labeled) (Figure 3); costoclavicular compression of the gray proton-dense fibrosis of the second division right of the subclavian artery with binding nerve trunks (not displayed). Anterior-rotated heads of the clavicle compressing the inferior bicuspid valve within the left internal jugular vein and the gray proton-dense right brachiocephalic vein against the first division of the artery against the dilated gray proton-dense right vertebral vein (Figure 4).

Coronal, transverse, transverse oblique, and sagittal sequences cross-referenced the follicular cystic right thyroid gland, residual left lobe of the thyroid gland, scarring over the site of left mastectomy, fibrosis of the right scalene triangle, and compressed subclavian veins, right greater than left.

The 2-dimensional time-of-flight MRA/MRV (Figure 5) displayed the splayed-apart great vessels by the enlarged lobe of the right thyroid gland displayed on the T1-weighted images, crimping of the great vessels, and the marked compression of the asymmetric external jugular veins as they drained in and over the compressed inferior bicuspid valves within the internal jugular veins at the junction of the brachiocephalic veins.

Coronal fast-spin echo sequence documented hepatic cysts (not labeled) and the high proton-dense mixed follicular degeneration of the right lobe of the thyroid downwardly displacing the crimped great vessels (Figure 6) with splaying apart of the carotid sheaths and the mixed signal intensities of clips over the resected left lateral chest wall (not labeled).

Bilateral abduction external rotation (AER) of the upper extremities (not displayed) capture images of enhanced costoclavicular compression, right greater than left, and triggered complaints of pain over the anterior right chest wall and pain back and forth over the right neck. Left-triggered complaints triggered pain within left axilla.

DISCUSSION

The term *goiter* refers to an enlarged thyroid gland not associated with overproduction of thyroid hormone or malignancy. The thyroid may be visualized as a mass in the neck. The enlargement of the thyroid gland may arise from a diet deficient in iodine and the increase in thyroid-stimulating hormone (TSH) responding to the decrease in normal hormone synthesis within the thyroid gland. The TSH from the pituitary causes the

Figure 3. Transverse image that cross-references the coronal sequence to display the follicular cystic right lobe of the thyroid (TH) splaying apart the crimped subclavian (SA) and common carotid arteries (CC)

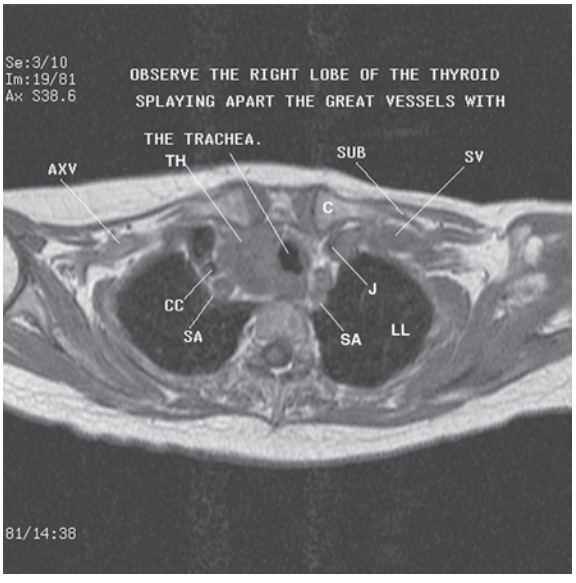

AXV, axillary vein; C, clavicle; J, left internal jugular vein; LL, left lung; SUB, subclavius muscle; SV, subclavian vein; T, trachea.

Figure 4. Left and right sagittal MR images (30/75 and 44/75). Image 30/75 displays the crimped left common carotid artery (CC) and the left internal jugular vein (J) compressed against vertebral vein (VV) as it drains into the left brachiocephalic vein (BRV), and the left subclavian artery (SA) mildly compressed as it enters the left scalene triangle. Observe image 44/75, which displays the follicular cystic right lobe of the thyroid gland (TH) downward-displacing the second division of the right subclavian artery (not labeled) against the dilated gray proton-dense right vertebral vein (VV).

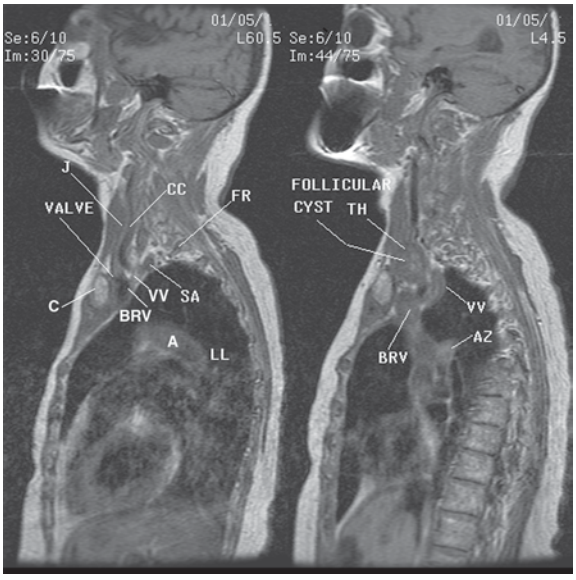

A, aorta; AZ, azygos vein; BRV, brachiocephalic vein; C, clavicle; FR, first rib; LL, left lung; Valve, inferior bicuspid valve within the left internal jugular vein.

thyroid to enlarge. The enlargement usually takes many years and eventually displaces/crimps the great vessels, as in our patient.[1] The trachea and esophagus are often displaced, triggering coughing and the sensation of food being stuck in the upper throat. Thyroid hormone pills may be given to treat small goiters by having the pituitary gland to produce less TSH, which should result in stabilization in size of the gland. This technique often will not cause the size of the goiter to decrease but usually keeps it from growing any larger. Patients who do not respond to thyroid hormone therapy are often referred for surgery. In 1964, isotope imaging of the thyroid gland often would display a "cold nodule" within an enlarged thyroid gland, which was suspicious for malignancy. A percutaneous biopsy would often be nondiagnostic. However, MRI displays so-called cold nodules as areas of fat necrosis consistent with decreased venous drainage.[2]

Thoracic outlet syndrome is a clinical diagnosis that results from laxity of the sling/erector muscles of the shoulder (serratus anterior, levator scapulae, trapezius).[3-6] Kyphosis of the thoracic spine occurs in thoracic outlet syndrome patients, increasing the slope of the first ribs backwardly displacing the manubrium that compresses the ascending aorta and crimps (like a water hose) the great vessels. High proton-dense fat necrosis within the thyroid gland is often displayed on T1-weighted MRI of thoracic outlet syndrome patients suspicious for hypothyroidism.[1] The posterior-anterior and lateral chest radiographs in our patient suggested an enlarged thyroid

Figure 5. Three-dimensional reconstructed 2-dimensional time-of-flight MRA/MRV image that displays the decreased signal intensities of the compressed subclavian veins (SV) asymmetric reciprocally dilated axillary veins (AXV) and the dilated right internal jugular veins, right greater than the left; compressed decreased signal intensities of the second divisions of the subclavian arteries (SA) (site of the binding nerve trunks).

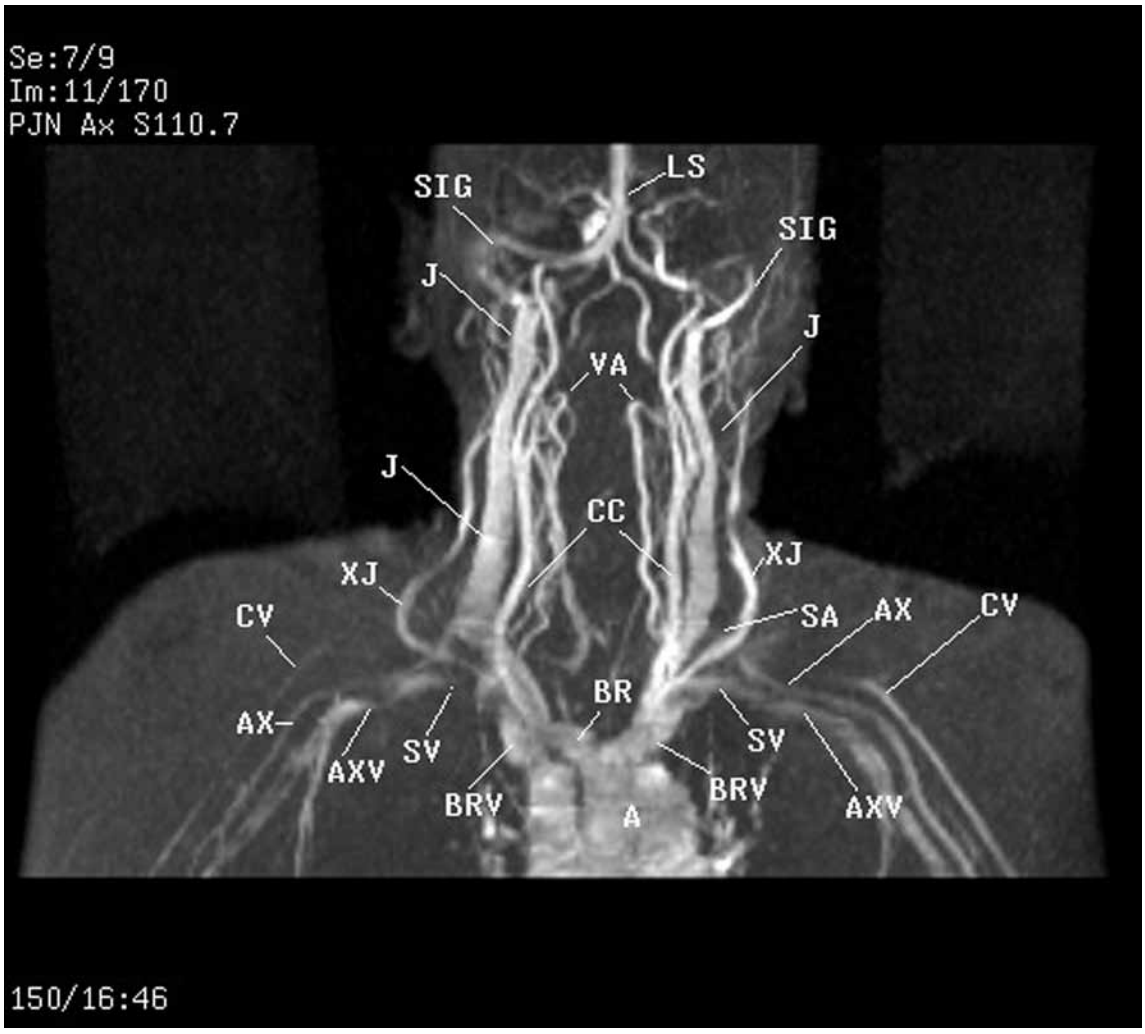

A, aorta; AX, axillary artery; BR, brachiocephalic artery; BRV, brachiocephalic vein; CV ,cephalic vein; CC, common carotid artery; XJ, external jugular vein; J, internal jugular vein; LS, longitudinal sinus; SIG, sigmoid sinus; VA, vertebral artery.

gland displacing the trachea to the left of midline.[4] Multiplanar MRI confirmed the above. The fast-spin echo sequence confirmed cystic fat necrosis within the right lobe of the thyroid gland. The follicular cystic right lobe of the thyroid gland and the backward manubrium splayed apart the great vessels, enhancing costoclavicular compression of the inferior bicuspid valves within the internal jugular veins impeding venous return from the draining veins within the neck.[7] The patient and requesting physician were immediately made aware of the above findings. Since not all of the images could be presented, those that best displayed the pathology were selected. A more detailed description of the above findings was provided to the requesting physician.

CONCLUSIONS

- Post–left mastectomy as above described;
- Postresected left lobe of the thyroid gland;
- Hepatic cysts;
- Follicular cystic large right thyroid gland enhancing crimping and splaying apart the great vessels;
- Fibrosis of the right scalene triangle into the supraclavicular fossa;
- Cervicothoracic lumbar kyphoscoliosis as above.
- Bronchiectasis left lung as above;
- No metastatic disease identified;
- Bilateral costoclavicular compression (laxity of the great vessels-trapezius, levator scapulae and the serratus anterior muscles) of the bicuspid valves within the draining veins of the neck,

Figure 6. Coronal fast-spin echo MRI that displays the high proton-dense follicular cysts within the right thyroid gland and high proton-dense hepatic cyst (not labeled).

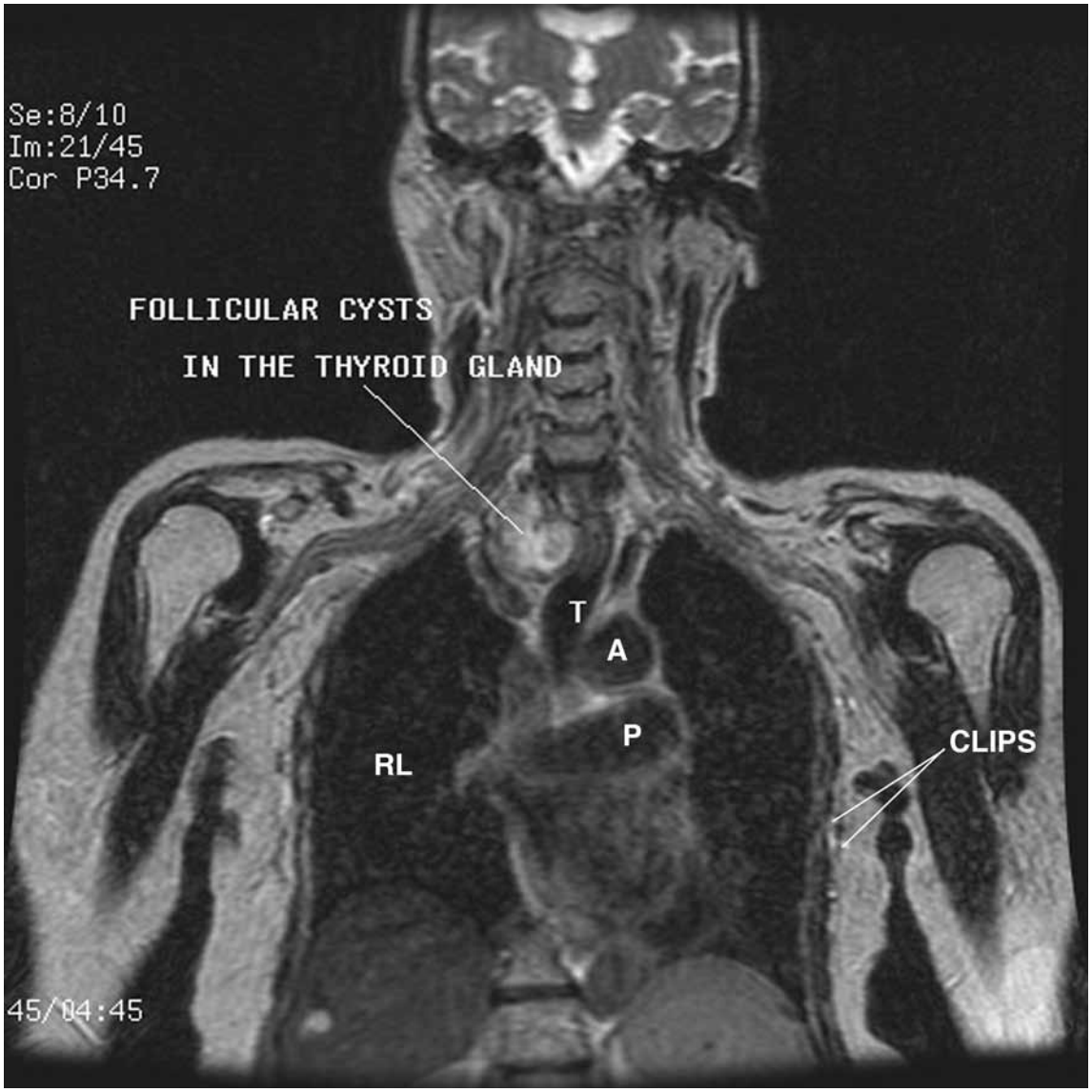

A, aorta; CLIPS, resected breast; P, pulmonary artery; RL, right lung; T, trachea.

supraclavicular fossae with lymphatics and compression of the subclavian and axillary arteries with binding nerves decreasing venous return from the brachial plexus and decreasing arterial flow to the brachial plexus as above described;
- Bilateral abduction external rotation of the upper extremities (AER) captured images and triggered complaints greater right than left as above described.

TAKE-HOME MESSAGE

Posterior-anterior and lateral chest radiographs are essential for examination of the thorax on MRI. The upright x-rays provide normal and abnormal landmark anatomy.[5,8] Knowledge of anatomy allows the radiologist to consider different etiologies in patient complaints. This was certainly the finding in our patient. Monitoring the MRI sequences at the console detected mixed signal intensities within the right lobe of the thyroid gland suggesting a cystic component. Single high proton-dense fat necrosis in the thyroid gland is not uncommon in thoracic outlet syndrome patients.[1] The fast-spin echo MRI sequence is excellent for displaying abnormal lymphatics in patients with lymphedema as well as fat necrosis within major organs.

ACKNOWLEDGEMENTS

Thanks to David Nelson, Steven Do, and Portia Daniels of the University of California Los Angeles Radiology Media Center.

REFERENCES

1. Collins JD, Shaver M, Disher A, Miller TQ. Compromising abnormalities of the brachial plexus as displayed by magnetic resonance imaging. *Clin Anat*. 1995;l8:1-16.

2. Collins JD. www.tosinfo.com. Accessed March 2011.

3. Lord JW, Rosati LM. Thoracic outlet syndromes. *Clinical Symposia Ciba Geigy*. 1971:1-32.

4. Collins JD, Shaver M, Batra P, Brown K, Disher A. Magnetic Resonance Imaging of Chest Wall Lesions. *J Natl Med Assoc*. 1991:4:352-360.

5. Woodburne, RT, Burkel WE. Essentials of Human Anatomy. 8th ed. New York, NY: Oxford University Press; 1988:18-216.

6. Atassoy E. Thoracic outlet compression syndrome. *Orthop Clin N Am*. 1996;27:265-303.

7. Sunderland S. Blood supply of the nerves to the upper limb in man. *Arch Neurol Psych*. 1945;53:91-115.

8. Clemente, CD. Anatomy, A Regional Atlas of The Human Body. 3rd ed. Baltimore, MD: Urban and Schwarzenberg; 1987. ■